Virology 278, 423–435 (2000)
doi:10.1006/viro.2000.0631, available online at http://www.idealibrary.com on IDEAL®

Two Influenza A Virus-Specific Fabs Neutralize by Inhibiting Virus Attachment to Target Cells, While Neutralization by Their IgGs Is Complex and Occurs Simultaneously through Fusion Inhibition and Attachment Inhibition

M. J. Edwards[1] and N. J. Dimmock[2]

Department of Biological Sciences, University of Warwick, Coventry CV4 7AL, United Kingdom

Received April 25, 2000; returned to author for revision June 1, 2000; accepted September 7, 2000; published online November 16, 2000

Mabs H36 (IgG2a) and H37 (IgG3) recognize epitopes in antigenic sites Sb and Ca2, respectively, in the HA1 subunit of influenza virus A/PR/8/34 (H1N1). Their neutralization was complex. Our aim here was to investigate the mechanism of neutralization by the IgGs and their Fabs. In MDCK and BHK cells, both IgGs neutralized primarily by inhibiting virus–cell fusion, although at higher IgG concentrations virus attachment to target cells was also inhibited. In contrast, the Fabs neutralized entirely by inhibiting virus attachment, although a higher concentration of Fab than IgG was required to bring this about. Both H36 and H37 exerted a concentration-dependent spectrum of neutralization activity, with virus–cell fusion inhibition and virus–cell attachment inhibition being the predominant mechanisms at low- and high-antibody concentration, respectively, and both mechanisms occurring simultaneously at intermediate concentrations. However, it may be that attachment inhibition was a secondary event, occurring to virus that had already been neutralized through inhibition of its fusion activity. Neutralization by H36 and H37 Fabs was a simple process. Both inhibited virus attachment but required much higher (>100-fold) molar concentrations for activity than did IgG. The functional affinities of the IgGs were high (0.4–0.6 nM) and differences between these and the affinity of their Fabs (H36, nil; H37, 23-fold) were not sufficient to explain the differences observed in neutralization. Similar neutralization data were obtained in two different cell lines. The dose–response curve for neutralization by H36 F(ab′)$_2$ resembled that for IgG, although eightfold more F(ab′)$_2$ was required for 50% neutralization. Overall, neutralization mechanisms of H36 and H37 antibodies were similar, and thus independent of antigenic site, antibody isotype, and target cell.

Key Words: influenza A virus; neutralization; IgG; Fab; F(ab′)$_2$; affinity; mechanism of neutralization; inhibition of attachment; inhibition of internalization; inhibition of fusion.

INTRODUCTION

Neutralization is an *in vitro* process in which virus binds antibody and loses infectivity (Dimmock, 1993). It correlates strongly, though not exclusively, with protection from infection *in vivo.* Exactly how the antibody brings about neutralization and what functions of the virion are inhibited during neutralization are poorly understood. However, it was previously established that neutralization is complex and multifactorial and, for any one virus, is governed by factors that include the virus strain, the epitope, the cell type, and the antibody isotype, affinity, and concentration. While it is never possible to show unequivocally how a virus is neutralized, loss of infectivity can, with care, be correlated with the loss of particular viral functions that are known to be essential in the initial stages of infection. To establish a putative causal relationship, however, loss of a particular virus function must be able to account quantitatively for the loss of infectivity as represented by the antibody dose–neutralization curve or kinetics of neutralization.

Although influenza A viruses are important human pathogens, their natural reservoir is aquatic birds (Webster, 1998). There are 135 subtypes defined by the permutation of the two major surface antigens, the hemagglutinin (HA; of which there are 15 antigenic forms) and the neuraminidase (of which there are 9), and each subtype contains many different strains. So far only 4 subtypes (H1N1, H2N2, H3N2, and H3N8) have spread in the human population, but there is serious concern for human health with viruses crossing the species barrier, such as the H5N1 in Hong Kong that recently caused 38% mortality (Centers for Disease Control and Prevention, 1998). The major neutralization antigen is the HA, and protection from infection in humans is due largely to humoral immunity (Ghendon, 1990).

Neutralization of viruses by Fabs is potentially a simpler process than neutralization by IgG, as Fabs can bind only monovalently to virions. Thus study of Fabs can help elucidate neutralization mechanisms. Most Fabs have at least an order of magnitude less neutralization activity on a molar basis compared with that of their IgG, although

[1] Present address: The Edward Jenner Institute for Vaccine Research, Compton RG20 7NN, UK.

[2] To whom correspondence and reprint requests should be addressed. Fax: +44 1 2476 523593. E-mail: ndimmock@bio.warwick.ac.uk.

0042-6822/00 $35.00

some neutralize more efficiently (Kingsford *et al.,* 1991; Stewart *et al.,* 1997). Fabs were classified into five categories according to their change in affinity and neutralizing ability relative to their parent antibody, but only in some cases was the difference between IgG and Fab neutralization explicable in terms of reduced Fab affinity (Schofield *et al.,* 1997b). Almost nothing is known about how Fabs neutralize influenza A viruses, and there is very little information about the mechanism of Fab neutralization of viruses in general. Neutralization of HIV-1 infection of the C8166 T-cell line by the human b12 Fab differed from that of its IgG1. While neither affected attachment of neutralized virus to the target cell sufficiently to account for neutralization (McInerney *et al.,* 1997; Ugolini *et al.,* 1997), the IgG inhibited fusion coordinately with neutralization, while its Fab neutralized virus without affecting its fusion activity (McInerney *et al.,* 1997).

Previous work showed that IgG neutralization of influenza A virus is complex and that loss of infectivity occurs in a variety of ways, depending on several different variables as discussed above. Neutralization did not (1) inhibit attachment of virus to the target cell (Possee and Dimmock, 1981; Possee *et al.,* 1982; Dimmock *et al.,* 1984; Taylor and Dimmock, 1985; Rigg *et al.,* 1989), and neutralized virus attached via neuraminidase-sensitive receptors (Outlaw *et al.,* 1990). With other virus strains and/or antibodies, neutralization was accompanied by (2) partial inhibition of virus to the target cell (Outlaw and Dimmock, 1990, 1993; Outlaw *et al.,* 1990. (3) Internalization of neutralized virus that attach to cells, however, was not inhibited (Outlaw *et al.,* 1990; Outlaw and Dimmock, 1993). There was also (4) partial inhibition of fusion activity of cell-associated virus (Outlaw and Dimmock, 1993), (5) complete inhibition of fusion activity of cell-associated virus (Outlaw and Dimmock, 1993), or (6) no inhibition of fusion. With the latter, neutralization was associated with inhibition of a postfusion event (Possee and Dimmock, 1981; Possee *et al.,* 1982; Dimmock *et al.,* 1984; Rigg *et al.,* 1989) and was also seen during neutralization by polymeric IgA (Armstrong and Dimmock, 1992). A combination of partial inhibition of attachment and partial inhibition of fusion (7) could theoretically have accounted for neutralization (Outlaw and Dimmock, 1993). Aggregation of virus (8) played only a minor role in reducing infectivity and was always restricted to a particular window of antibody concentration (Outlaw and Dimmock, 1990; Outlaw *et al.,* 1990).

We report here on the mechanism of neutralization of an H1N1 influenza A virus by an HA1-specific monoclonal IgG2a and an IgG3, and their Fabs. In MDCK and BHK cells, both IgGs neutralized primarily by inhibiting virus–cell fusion, although at higher IgG concentrations virus attachment to target cells was also inhibited. In contrast, the Fabs neutralized entirely by inhibiting virus attachment, but a higher concentration of Fab than of IgG was required to bring this about.

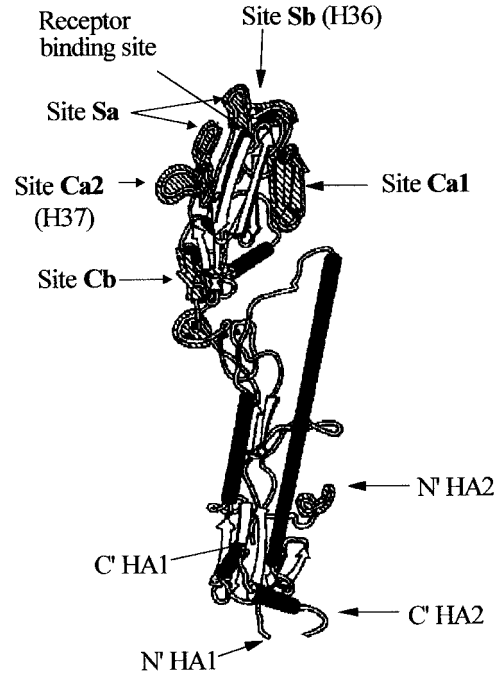

FIG. 1. Location of the antigenic sites of Mabs H36 and H37 on a monomer of the HA of PR8 (adapted from Wiley *et al.* (1981) and Caton *et al.* (1982)).

RESULTS

Location of epitopes of Mabs H36 and H37 on the viral hemagglutinin

Mab H36 (IgG2a) binds to an epitope in antigenic site Sb at the distal tip of the HA1 subunit that equates to site B of the H3 HA, and H37 (IgG3) binds to site Ca2, which encompasses a loop on the globular head of HA1 that equates to site A of the H3 HA (Fig. 1) (Caton *et al.,* 1982; Staudt and Gerhard, 1983). RT-PCR and sequencing of neutralization escape mutants implied that there were single residue changes in the expected antigenic sites. With H36 IgG the majority of escape mutants had 152D → K, and with H37 IgG the majority had 140K → D (A. C. Marriott, C. Parry, and N. J. Dimmock, unpublished data).

Neutralization efficiencies of H36 IgG, F(ab′)$_2$ and Fab, and H37 IgG and Fab

Figure 2a shows that H36 IgG, F(ab′)$_2$, and Fab all gave >99% neutralization of virus infectivity, but neutralization efficiency decreased in the order IgG > F(ab′)$_2$ > Fab. Curves were fitted by nonlinear regression analysis and neutralization efficiencies were calculated. These showed that 50% neutralization (N_{50}) required 8-fold more F(ab′)$_2$, in molar terms, and 104-fold more Fab (Table 1). Interestingly this differential decreased with increasing neutralization, such that N_{90} required 2.5-fold more F(ab′)$_2$ and 15-fold more Fab than IgG. Fab neutralization

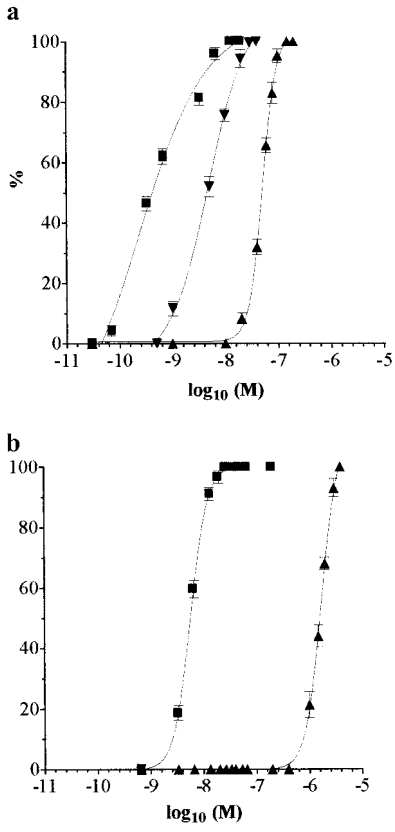

FIG. 2. Dose–response relationship of the percentage infectivity of PR8 remaining after incubation with increasing concentrations of Mabs (a) H36 and (b) H37 for 1 h at 37°C. IgG, (■); $F(ab')_2$, (▼); Fab, (▲). Virus controls gave approximately 40 PFU/plate. Data are from plaque assays in MDCK cells and are the means of three experiments each with five replicates. Bars represent the SEM. Curves ($R > 0.98$) were generated by nonlinear regression analysis using Prism Graphpad software.

occurred over a narrower concentration range than did IgG neutralization. Neutralization by Mab H37 was essentially similar to that of H36 IgG, except that approximately 10-fold more H37 IgG was required for N_{50} than with H36 IgG and that H37 IgG achieved >99% neutralization over a narrower concentration range than did H36 IgG (Figs. 2a and 2b). H37 Fab was also neutralizing, though the N_{50} required approximately 360-fold more than did the IgG. As H37 IgG is completely degraded by pepsin, its $F(ab')_2$ could not be studied. Again H37 showed a differential in the ratio of IgG:Fab required for N_{50} and N_{90}, although of only 2-fold. Similar data were obtained when neutralization assays were conducted in BHK cells (data not shown).

H36 and H37 IgG neutralized more infectivity than could be accounted for by inhibition of virus attachment to the target cell

Dose–response curves are shown for neutralization and inhibition of virus attachment to cells for a range of H36 and H37 IgG and Fab concentrations in MDCK and BHK cells. IgG and Fab data are based on 20 and 12 replicate assays, respectively. Neuraminidase pretreatment of the target cell monolayer reduced the level of attachment of both nonneutralized and neutralized virus by >90%, showing that both used NANA receptors and that binding to Fc receptors was not involved. In all cases, attachment of virus decreased with increasing neutralization, although the correlation between the curves for H36 IgG was poor (Figs. 3a and 3b), as determined by an unpaired *t* test, showing that they were significantly different ($p = 0.001$ and 0.005, respectively, where 0.05 is considered significant). The H37 curves followed the same trend and, although the difference was not so marked, they were still significantly different ($p = 0.027$ and 0.047, respectively; Figs. 3c and 3d). At N_{50}, there was only 5–20% inhibition of attachment, indicating that the majority of virus was neutralized by some other mechanism (Table 2). Inhibition of attachment increased, however, relative to neutralization with increasing IgG concentration, so that at N_{90} inhibition of virus attachment accounted for the majority of the observed neutralization (summarized in Table 2). The comparison of neutralization and inhibition of attachment is legitimate, as we used the same experimental system, same sized monolayers, same virus–antibody mix, and same inoculum volume, etc., for both assays.

The H36 and H37 Fab data were in marked contrast to the data obtained with their IgGs, as the neutralization and inhibition of virus–cell attachment curves were virtually superimposable (Figs. 3e–3h) and did not differ significantly by the unpaired *t* test (values shown in Fig. 3). All required ≥86-fold more Fab than IgG for equivalent neutralization. Thus Fab neutralization and inhibition of virus attachment appeared to be causally related. H36 Fab showed a much steeper dose–response curve than did H36 IgG (compare Figs. 3a and 3b with 3e and 3f; Fig. 2a). All aspects of the ELISA and the plaque assay

TABLE 1

Comparison of the Neutralizing Activities of H36 and H37 IgG and Their Antibody Fragments in MDCK Cell Monolayers

	Concentration (nM) required to give neutralization of		Antibody fragment:IgG ratio at neutralization of	
Antibody	50%	90%	50%	90%
H36				
IgG	0.5	6.0		NA
$F9(ab')_2$	4.0	15.0	8:1	2.5:1
Fab	52.0	90.0	104:1	15.0:1
H37				
IgG	5.0	14.0		NA
Fab	1800.0	2500.0	360:1	178.0:1

Note. Plaque assay data from Fig. 2.

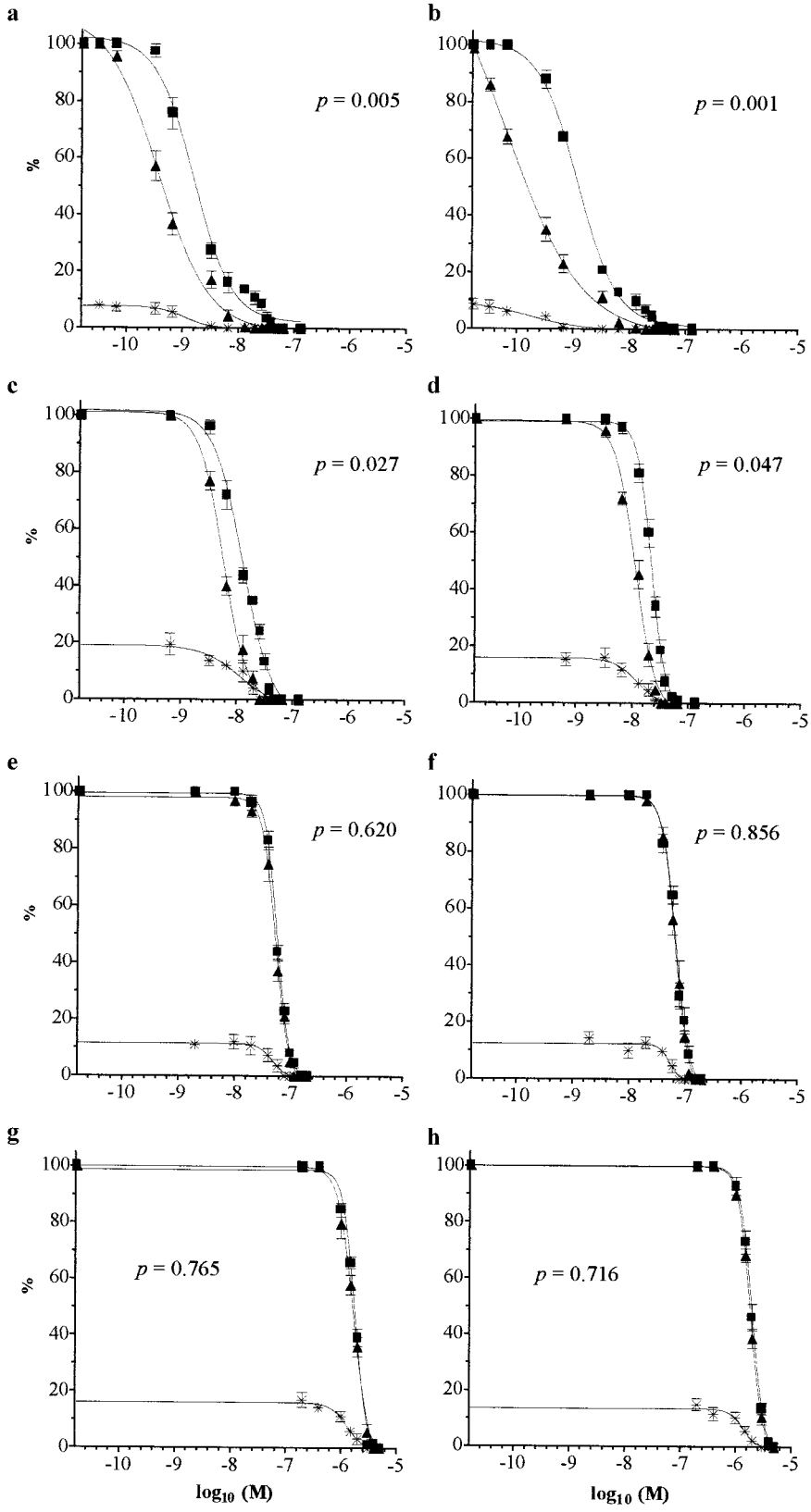

FIG. 3. Dose–response relationship between the percentage infectivity and percentage attachment of virus to MDCK (a, c, e, g) and BHK cells (b, d, f, h) as a function of IgG and Fab concentration. Data are for H36 IgG (a, b), H36 Fab (e, f), H37 IgG (c, d), and H37 Fab (g, h). Infectivity and attachment were assayed in parallel by ELISA in the same batch of monolayers in 96-well plates, using the same virus–antibody mixtures. Virus and antibody were incubated together for 1 h at 37°C. ▲, percentage infectivity; ■, percentage attachment of virus to cells; *, percentage attachment of virus to cells pretreated with *Clostridium perfringens* neuraminidase. Data with IgG are the means of five experiments each with four replicates, and for Fab

TABLE 2

Summary of Some Parameters of the Neutralization of PR8 by the HA1-Specific H36 and H37 IgGs and Their Fabs

Mab	Isotype	Antigenic site	Cell type	N_{50}[a] (nM)		Inhibition (%) of attachment at N_{50}		Inhibition (%) of attachment at N_{90}		Inhibition of virus internalization by IgG	Inhibition of virus fusion by IgG
				IgG	Fab	IgG	Fab	IgG	Fab		
H36	G2a	Sb (tip)	MDCK	0.6	52	12	42	73	88	No	Yes
			BHK	0.2	63	5	49	70	85	No	Yes
H37	G3	Ca2 (loop)	MDCK	5.0	1600	20	42	65	88	No	Yes
			BHK	10.0	1800	10	48	61	85	No	Yes

[a] N_{50}, 50% neutralization by ELISA.

neutralization data shown in Figs. 3 and 2 were comparable.

In conclusion, neutralization by H36 and H37 Fabs appeared to be a simple process, related directly to the inhibition of virus attachment to the target cell, whereas IgG neutralization was complex and involved the inhibition of at least two virus activities. Counterintuitively, H36 IgG neutralized the majority of the virus population at low concentration by a mechanism other than the inhibition of virus attachment. Possible reasons that the Fabs required an 87- to 320-fold higher molar concentration than IgG for 50% neutralization are discussed below.

H36 and H37 IgG-neutralized virus that attached to target cells was internalized

The next phase of the study investigated whether neutralized virus that attached to target cells had the ability to be internalized by those cells. After it attaches to the target cell, influenza virus undergoes receptor-mediated endocytosis. This was verified in our system by two treatments that reduce receptor-mediated endocytosis. Cells were either chilled at 4°C (Matlin *et al.,* 1981; Richman *et al.,* 1986) or pretreated with medium made hypertonic with sucrose (Daukas and Zigmond, 1985; Heuser and Anderson, 1989). For example, internalization of nonneutralized or H36-neutralized virus into MDCK cells was inhibited by ≥92% at 4°C and by ≥81% by hypertonic medium. Similar data were obtained for BHK cells and in other experiments (data not shown). Figures 4a and 4b show data for a full range of IgG concentrations. It can be seen that, as infectivity decreased with increasing concentration of H36 or H37 IgG, internalization of virus by MDCK cells remained at approximately 100%, and thus was independent of the amount of neutralization. The data shown represent only the virus that attached to cells (see Materials and Methods). Similar data were obtained with BHK cells (not shown). Thus virus neutralized by H36 or H37 IgG that was able to attach to cells was also able to undergo internalization by the target cell.

H36 and H37 IgG neutralized infectivity and inhibited the fusion of virions to target cells in parallel

Infection of cells at 37°C with R18-labeled virus results in fluorescence dequenching consistent with fusion of virus and cell membranes, as reported by others for a variety of virus systems (Blumenthal *et al.,* 1987; Stegmann *et al.,* 1987; Miller and Hutt-Fletcher, 1988; Haddad and Hutt-Fletcher, 1989; Outlaw and Dimmock, 1993). The specificity of this result was confirmed by treatments that inhibit PR8 virus fusion. Cells were either chilled at 4°C (Tsurudome *et al.,* 1992; Pak *et al.,* 1994) or pretreated with bafilomycin, a V-ATPase inhibitor that prevents the acidification of endosomal vesicles required for triggering HA-mediated fusion (Palokangas *et al.,* 1994; Ochiai *et al.,* 1995). Preincubating MDCK cells at 4°C inhibited fusion by 91 ± 3%, while treatment with bafilomycin inhibited virus fusion by 88 ± 5% (other data were similar but not shown). Figures 5a–5d show the relationship between IgG neutralization and virus fusion activity in MDCK and BHK cells. Fusion data were calculated relative to the percentage of virus that attached to cells, measured in the same system (see Materials and Methods). Data show that, as infectivity decreased with increasing IgG concentration, the percentage fusion curves followed very closely, suggesting a causal relationship. Although the two curves were not perfectly superimposable, they did not differ significantly by an unpaired *t* test (see Fig. 5 for *p* values). Thus the majority of virus that was neutralized by H36 and H37 IgG and attached to target cells resulted from inhibition of virus–cell fusion.

three experiments each with four replicates. Virus controls gave readings of 1.2–1.4 OD units. The bar represents the SEM. Curves ($R > 0.98$) were generated as described in Fig. 2. The *p* values showing the significance of the difference between the two curves (▲, ■) were calculated using an unpaired *t* test. A value of $p < 0.05$ is considered significant.

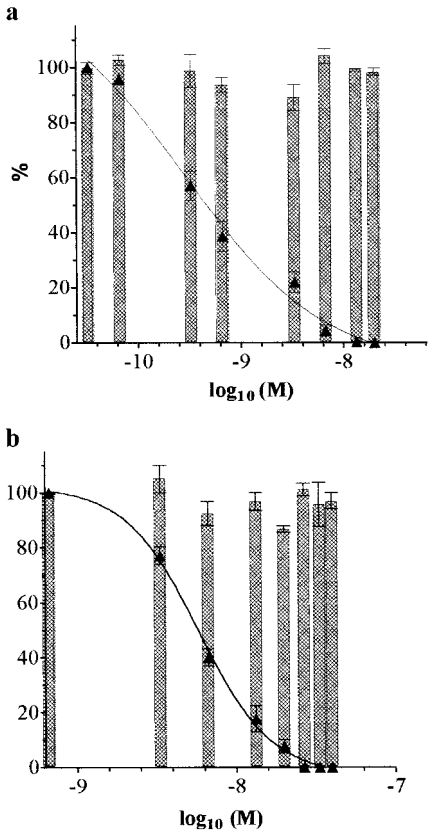

FIG. 4. Analysis of the relationship between the infectivity of PR8 and the internalization of virus by MDCK cells as a function of H36 (a) and H37 (b) IgG concentration. Virus and antibody were incubated together for 1 h at 37°C. Infectivity and internalization were assayed by ELISAs in the same batch of monolayers in 96-well plates, and using the same virus–antibody mixtures. ▲, percentage infectivity; columns represent percentage internalization. All data are the means of three experiments each with four replicates. Internalization was calculated as a percentage of virus that attached to cells, measured in the same system. Virus controls gave readings of 0.7–1.0 OD units. The bar represents the SEM.

H36 F(ab′)$_2$ neutralized more infectivity than could be accounted for by inhibition of virus attachment to the target cell

Figure 6 shows the relationship between F(ab′)$_2$ neutralization and the inhibition of attachment of virus to target cells. Neuraminidase pretreatment reduced the level of virus attachment by >85%, showing that most virus attached via NANA receptors. Like the IgG neutralization shown in Fig. 2a, a progressively greater proportion of virus neutralization could be accounted for by inhibition of attachment as the concentration of F(ab′)$_2$ increased. For example, inhibition of virus attachment at N_{50} was only 2% and at N_{90}, 78%. Thus, although F(ab′)$_2$ has an eightfold lower specific activity than its IgG, they both appeared to neutralize in a similar manner. Possible reasons for the lower neutralizing activity of F(ab′)$_2$ are discussed below.

Measurement of functional affinities of IgGs and affinities of their Fabs

The on- and off-rates for H36 and H37 IgGs and their Fabs for immobilized whole virus were measured using surface plasmon resonance, and the functional affinities and affinities calculated, respectively. The on- and off-rates of H36 IgG and Fab were very similar and the equilibrium values were high and identical. H37 Fab had a 2-fold lower on-rate and a 7-fold higher off-rate than its IgG, and its equilibrium value was 23-fold lower (Table 3). However, all equilibrium values were approximately 9 nM or better, which is the high end of the range for antibodies.

DISCUSSION

Neutralization by IgG

On a molar basis, H36 IgG had an approximately 10-fold higher neutralizing activity than H37 IgG. Neutralization by both Fabs was considerably reduced (by 87- to 320-fold at 50% neutralization [N_{50}]). More surprising was the 8-fold lower activity of the H36 F(ab′)$_2$. Inhibition of virus attachment to target cells did not appear to account for all the neutralization observed. For example, the N_{50} of H36 and H37 IgGs in MDCK cells and BHK cells was accompanied by inhibition of virus attachment that ranged from 5 to 20% (a 10- to 2.5-fold discrepancy; Table 2). This result was highly reproducible in five repeat experiments and four replicate assays in each (Figs. 3a–3d). Thus, how the majority of virus lost infectivity was still unexplained. In an attempt to resolve this, we investigated the next stages of infection, virus internalization and virus fusion. We found that neutralized virus that attached to cells was internalized with the same overall efficiency as nonneutralized virus (Fig. 4), but that fusion was inhibited in proportion to neutralization by both H36 and H37 IgGs (Fig. 5). We thus concluded that both IgGs neutralized the majority of virus by inhibiting viral fusion and that underlying this was a low level of inhibition of virus attachment. What made this situation complex was that, as higher concentrations of IgG were applied, attachment inhibition increased compared with fusion inhibition and eventually became the major mechanism of neutralization.

From the above-noted observations and results we conclude, first, that neutralization mechanisms effected by H36 and H37 IgGs proceed in much the same way and are thus unaffected by differences in antibody isotype (IgG2a and IgG3), antigenic site (Sb and Ca2), or epitope. At the N_{50}, H37 IgG was 10-fold less efficient at neutralizing in molar terms. This was not explained by its functional affinity, which was 1.4-fold higher than that of H36 IgG (Table 3), but may have resulted from the proximity of its antigenic site to the receptor-binding site (Fig. 1). Thus the H37 epitope appears to give intrinsically less

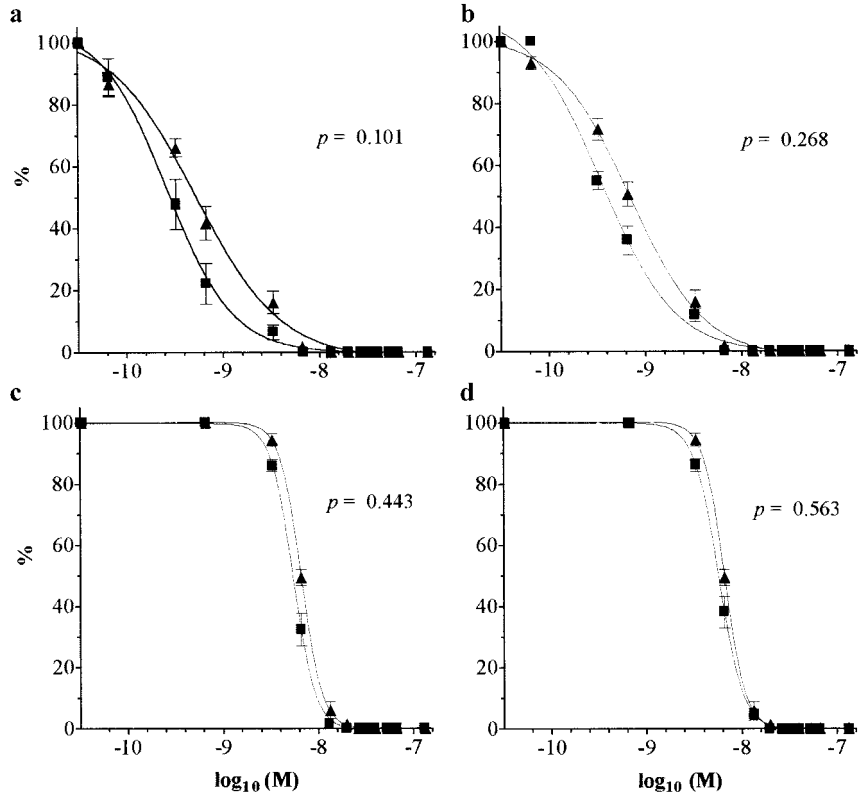

FIG. 5. Analysis of the relationship between the percentage infectivity of PR8 and the percentage fusion of virus to MDCK (a,c) and BHK (b,d) cells as a function of antibody concentration. H36 IgG (a, b); H37 IgG (c, d). Both sets of data were obtained using 3-cm-diameter monolayers. Virus and antibody were incubated together for 1 h at 37°C. Percentage infectivity (▲) was determined by plaque reduction (virus controls gave approximately 40 PFU/plate), and percentage inhibition of fusion activity (■) was measured by fluorescence dequenching of R18-labeled virus. The ratio of virus control to background fluorescence was ≥threefold. Data are the means of three experiments each with three replicates. Fusion was calculated as a percentage of virus that attached to cells, measured in the same system. The bar represents the SEM. Curves ($R > 0.98$) were generated as described in Fig. 2, and p values showing the significance of the difference between the two curves were calculated using an unpaired t test. A value of $p < 0.05$ is considered significant.

neutralization per IgG molecule than does the H36 epitope. Indeed, a similar conclusion was reached earlier with a different combination of influenza A virus and Mab (Schofield *et al.,* 1997a). Second, it is evident that H36 and H37 IgGs exert two different neutralization mechanisms, inhibition of fusion and inhibition of attachment, that operate simultaneously. This suggests that IgG inhibits fusion at a lower density of IgG molecules per virion than is required for inhibition of attachment or, from the virus perspective, that fusion requires a higher number of free HA spikes than does cell attachment. However, direct quantitation is required to take this tentative conclusion further. Third, the proportion of virus putatively neutralized by inhibition of attachment rose with increasing antibody concentration. We speculate that this occurs because the number of IgG molecules bound per virion increases and, as a result, interaction of the virion with cell receptors is more effectively impeded. It is probably also the case that such virus was already neutralized through inhibition of its fusion activity, and that the extra IgG is simply inhibiting the attachment of already noninfectious virus. Which mechanism should be cited as the primary cause of neutralization? The logic is straightforward. Fusion inhibition is predominant at lower IgG concentrations, while attachment inhibition is a secondary event, requiring more IgG molecules per virion. However, when virus no longer attaches to target cells, fusion inhibition becomes irrelevant to neutralization; thus, there is a spectrum of neutralization activity which starts with fusion inhibition and ends with attachment inhibition. In between, both mechanisms of neutralization operate simultaneously, and the proportion of infectivity that each neutralizes depends on the concentration of IgG applied.

H36 and H37 are a further addition to a group of HA1-specific antibodies that inhibit influenza A virus-mediated fusion (Kida *et al.,* 1985; Outlaw and Dimmock, 1993). The Kida antibodies inhibited two different low-pH-induced conformational changes in soluble HA, as shown by electron spin resonance, but no quantitative link with neutralization or virus-directed fusion was established (Yoden *et al.,* 1986). Thus it is not clear how any of the antibodies are able to inhibit the fusion process. The main requirement for HA1 in the fusion process is

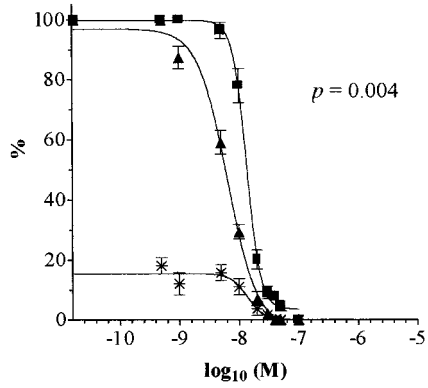

FIG. 6. Analysis of the relationship between infectivity and attachment of PR8 to MDCK target cells as a function of the concentration of H36 F(ab′)$_2$. Infectivity and attachment were assayed by ELISA in parallel in the same batch of monolayers in 96-well plates, using the same virus–antibody mixtures. Virus and antibody were incubated together for 1 h at 37°C. ▲, percentage infectivity; ■, percentage attachment of virus to cells; *, percentage attachment of virus to cells pretreated with *Clostridium perfringens* neuraminidase. Data are the means of three experiments each with three replicates. Virus controls gave readings of 1.2–1.4 OD units. The bar represents the SEM. Curves ($R > 0.99$) were generated as described in Fig. 2, and the p value showing the significance of the difference between the two curves (▲, ■) was calculated from an unpaired t test. A value of $P < 0.05$ is considered significant.

that it avoids impeding the low-pH-activated HA2 from making contact with the cell membrane (Hernandez *et al.,* 1996). The interpretation of how H36 and H37 act is made more difficult as they recognize different antigenic sites on HA1 (H36: site Sb (B); H37: site Sa (A); Fig. 1). Thus inhibition of fusion is not site-specific. We offer two possible explanations. In the first, IgG interferes sterically with the fusion process, possibly by keeping the viral and cell membranes apart. In the second, IgGs inhibit fusion by preventing the three HA1 monomers from moving out of the way of the low-pH-activated HA2 as it jackknifes toward the cell membrane (Bullough *et al.,* 1994). It seems unlikely that this is achieved by IgG's cross-linking two monomers within an HA trimer, as this is not observed by electron microscopy (Wrigley *et al.,* 1977, 1983), but could be achieved by cross-linking two adjacent HA trimers. However, all HA1 neutralization epitopes are conformational and many are discontinuous, so inhibition of fusion might be equally achieved by intraepitope cross-linking under the antibody footprint.

Neutralization by Fab

It is striking that the dose–response curves for inhibition of attachment and neutralization caused by both H36 and H37 Fabs were essentially identical, although a higher concentration of H37 Fab was needed (Figs. 3e–3h; Table 2); a causal relationship is thus strongly suggested. At first sight this seems counterintuitive, as a Fab (approximately 50,000 M_r) is threefold smaller than IgG (approximately 150,000 M_r) and would appear to be less able to sterically interfere with the binding of virus to cell receptors. However, the specific neutralization activities of H36 and H37 Fabs are two orders of magnitude lower than those of their respective IgGs, and it is possible that this arises because inhibition of attachment by Fab is the neutralization mechanism and that this requires a large number of Fab molecules bound per virion. The answer does not appear to lie with affinity for H36 Fab and IgG, as they have the same high value (0.56 nM), and, although the affinity of H37 Fab was 23-fold lower than that of its IgG, it was still high (9 nM) and would not account for the observed loss of infectivity. Thus the loss in affinity does not explain the observed loss of Fab neutralization activity. Rather, it would appear that H36 and H37 Fabs have lost much of the fusion-inhibition ability. However, if Fabs had simply lost fusion-inhibiting activity, one would expect the attachment inhibition curves of Fab and IgG to overlap. However, comparison of Figs. 3a–3d and 3e–3h shows this is not the case. Specifically, $10^{-7.5}$ M H36 IgG gave >90% neutralization, but at the same concentration, Fab neutralization was only just commencing. Moreover, in other experiments we showed that both H36 and H37 Fabs have the ability to inhibit postattachment stages of the virus–cell interaction (data not shown). They were able to neutralize virus already attached to cells, inhibit fluorescence dequenching when target cells were infected with R18-labeled virus, and inhibit the hemolysis of red blood cell–virus complexes (data not shown). Fabs therefore have not totally lost fusion-inhibiting activity, but carry this out less efficiently than IgG. Thus it appears that neutralization in general and fusion-inhibition in particular are more efficiently exerted by IgG than Fab because IgGs either bind bivalently or have a greater mass, or both. In summary, Fabs were less efficient than IgG at inhibiting virus attachment and were even poorer at inhibiting virus-mediated fusion; it is not yet clear why this is so.

No other data on the mechanism of neutralization of influenza A virus by Fabs are available. Early work

TABLE 3

Functional Affinities of H36 and H37 IgGs and Affinities of Their Fabs for Virus Particles Determined by Surface Plasmon Resonance

Antibody	On-rate constant (M^{-1} s^{-1})	Off-rate constant (s^{-1})	Equilibrium dissociation constant (nM)
H36			
IgG	5.88×10^5	3.24×10^{-4}	0.56
Fab	7.38×10^5	3.75×10^{-4}	0.56
H37			
IgG	4.25×10^5	1.59×10^{-4}	0.39
Fab	2.48×10^5	2.22×10^{-3}	9.0

Note. Values are the means of four different antibody concentrations.

showed that Fabs made from a polyclonal neutralizing IgG were neutralizing, but underwent the dilution dissociation that is normally indicative of a low-affinity association (Lafferty, 1963). Later it was shown that four Fabs to an H7N7 strain lost 31- to >100-fold neutralizing activity compared to their IgGs (Kida *et al.,* 1985). The mechanism of neutralization of another virus, HIV-1 infection of the C8166 T-cell line by the human b12 Fab, differed from that of its IgG1 (McInerney *et al.,* 1997). Neither inhibited attachment of neutralized HIV-1 to the target cell significantly, but b12 IgG inhibited fusion coordinately with neutralization, while its Fab neutralized without affecting fusion and presumably inhibited a post-fusion entry event. Another study found that both b12 IgG and Fab had some inhibitory effect on attachment of HIV-1 to the target cell, but the dose–response relationship for attachment inhibition was disproportionately less than that for the observed neutralization, demonstrating that there was not a direct causal relationship (Ugolini *et al.,* 1997).

Schofield *et al.* (1997b) classified Fabs into five categories according to their affinity and neutralizing ability. The H36 and possibly H37 Fabs described here clearly fall into their Category (iii), in which reduction in neutralizing activity exceeded loss of affinity by over 10-fold. This category also includes Fabs specific for mouse hepatitis virus (Lamarre and Talbot, 1995) and an influenza A H7N1 virus (Schofield *et al.,* 1997b).

Neutralization by F(ab′)$_2$

The specific neutralization activity of H36 F(ab′)$_2$ was reduced eightfold compared with that of its IgG, slightly greater than that found with F(ab′)$_2$ molecules specific to other viruses (Lamarre and Talbot, 1995; Schofield *et al.,* 1997b). This is unexpected, as a F(ab′)$_2$ is identical to IgG in valency and epitope binding site and differs only in the loss of the Fc region. This finding therefore adds weight to the above-noted suggestion that a higher mass of the neutralizing ligand makes for more-efficient neutralization. However, apart from requiring a greater concentration to effect neutralization, the relationship between neutralization and inhibition of virus attachment of F(ab′)$_2$ was similar to that of IgG described above. That is, there is insufficient inhibition of attachment at low F(ab′)$_2$ concentrations to explain the observed neutralization.

MATERIALS AND METHODS

Virus

Influenza virus A/Puerto Rico/8/34 (H1N1; PR8) was grown in the allantoic cavity of 10-day-old embryonated chicken eggs (Poynden Egg Farm, Goss Oaks, UK) for 48 h at 33°C. Virus was purified by differential centrifugation and then by banding successively on a 10–45% (w/v) sucrose gradient at 60,000 *g* for 90 min and a 20–70% (w/v) sucrose equilibrium gradient at 60,000 *g* for 16 h. Virus was stored at −70°C.

Cells

Madin–Darby canine kidney (MDCK) cells (kindly provided by Dr. Wendy Barclay) were maintained in DMEM (GibcoBRL Life Technologies, Paisley, UK), 0.02 mM glutamine (Gibco), 5% v/v heat-inactivated fetal calf serum (HIFCS; Gibco), and 50 μg/ml gentamicin (Gibco). BHK cells (ECACC, Porton Down, UK) were cultured in the same way but in GMEM (Gibco), 0.02 mM glutamine, 10% HIFCS, and 50 μg/ml gentamicin. Mouse hybridoma cell lines were grown in RPMI 1640 (Gibco), 10% HIFCS, 2 mM glutamine, and 50 μg/ml gentamicin.

Antibodies

The PR8 HA1-specific Mabs H36-4.5-2 (antigenic site Sb, IgG2a) and H37-45-5R3 (site Ca2, IgG3) were generously donated by Dr. Walter Gerhard (Caton *et al.,* 1982; Staudt and Gerhard, 1983). Another HA1-specific Mab H37-66-1 (site Sb, IgA) and an NP-specific Mab HB-67 (IgG1) were kindly supplied by Dr. Gerhard and Dr. Robert G. Webster, respectively. Mabs were purified by affinity chromatography on a protein A–Sepharose column (Sigma, Poole, UK) under low-salt conditions. IgG was eluted with 100 mM glycine (pH 3) and fractions were neutralized with 1 M Tris–HCl (pH 8). Peak fractions were concentrated with an Amicon 8010 pressure concentrator (Amicon, Stonehouse, UK) with a 10,000 M_r cutoff filter, dialyzed against PBS, and quantitated by UV absorption (1 OD = 1.35 mg/ml) (Harlow and Lane, 1988).

Production of Fabs by digestion of IgG with papain

IgG2a (1 mg) was mixed with 6.2 μl freshly made 0.01 M cysteine (Sigma), 20 μl EDTA, and 1 U agarose-immobilized papain (Sigma) and adjusted to pH 5.5 with 200 mM sodium acetate in a final volume of 1 ml. This was shaken for 3 h at 37°C. IgG3 was treated similarly except with 1 M cysteine. The reaction was stopped by pelleting the papain, making the digest 5.5 mM with respect to iodoacetamide (Sigma), and raising the pH with 1 M Tris–HCl (pH 8). The digest was passaged repeatedly through protein A–Sepharose to remove undigested IgG and Fc fragments. Fabs were then dialyzed, concentrated, and quantitated spectrophotometrically (1 OD = 1.5 mg/ml) (Hudson and Hay, 1989). The Fab preparation was then analyzed by nonreducing PAGE and stained with colloidal Coomassie brilliant blue (Sigma) (Fig. 7). It had the expected M_r of approximately 50,000 and was free of detectable IgG (≤50 ng/ml).

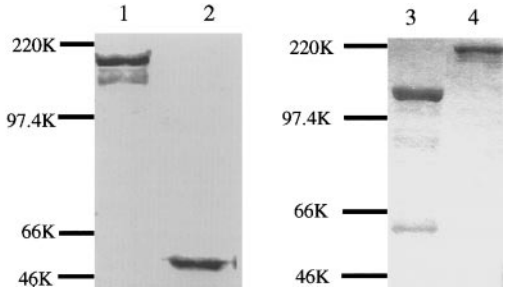

FIG. 7. Analysis of H36 antibody fragments by nondenaturing SDS–PAGE. Fab (10 μg) was analyzed on an 8% gel (left panel) and F(ab′)$_2$ (10 μg) on a 10% gel (right panel). Gels were stained with colloidal Coomassie Brilliant Blue. Lane 1, IgG; lane 2, Fab; lane 3, F(ab′)$_2$; lane 4, IgG. The positions of marker proteins are indicated.

Production of F(ab′)$_2$ by digestion of IgG2a with pepsin

H36 IgG2a (0.5 mg) was digested with 500 U immobilized pepsin (Sigma) at pH 3.5 for 8 h at 37°C. The reaction was stopped by pelleting the pepsin and raising the pH with 3 M Tris–HCl (pH 8). Undigested IgG was removed by passage through protein A–Sepharose. F(ab′)$_2$ was then dialyzed and concentrated, and its concentration was determined spectrophotometrically. By nonreducing SDS–PAGE, the F(ab′)$_2$ had the expected M_r of approximately 100,000 and was free of detectable IgG (≤50 ng/ml; Fig. 7). H37 IgG3 was degraded by pepsin and yielded no F(ab′)$_2$.

Hemagglutination assay

Virus was double diluted in PBS in 96-well round-bottom plates (Greiner, Stonehouse, UK) and detected by agglutination of 0.13% chicken red blood cells (CRBC; Serotech, Kidlington, UK). Agglutination of 50% (1 HAU) was estimated by interpolation between complete agglutination and no agglutination and the titer expressed as the reciprocal of the dilution in HAU/ml.

SDS–PAGE of proteins

SDS–PAGE was carried out on 8, 10, or 12% polyacrylamide gels with 10 μg protein. Samples were boiled for 3 min in nonreducing loading buffer. After electrophoresis, gels were fixed with 40% methanol, 10% acetic acid, and stained with colloidal Coomassie brilliant blue. IgG was detected down to 50 ng/ml.

Plaque assay of virus infectivity

MDCK monolayers were grown overnight on six-well plates (Falcon; Farenheit Lab Supplies, Milton Keynes, UK) followed by rinsing to remove serum, after which virus (100 μl) was added and incubated for 45 min at 20°C. Monolayers were then overlaid with 0.9% agar (Gibco) in 199 medium buffered with sodium bicarbonate, containing 0.2% (w/v) bovine serum albumin (BSA), 0.01% (w/v) DEAE dextran, 100 U/ml penicillin, 100 μg/ml streptomycin, and 30 U/ml TPCK trypsin (all from Sigma). After incubation for 3 days at 33°C, monolayers were fixed with formal-saline and stained with toluidine blue (BDH; Merck, Lutterworth, UK) for plaque counting.

Neutralization assay

Two methods were used. In the first, reduction in plaque number was determined. Virus (100 PFU/ml) was mixed with an equal volume of a range of dilutions of Mab for 60 min at 37°C, and then inoculated onto MDCK or BHK monolayers as described above. Neutralization was calculated as a percentage of the virus control and subtracted from 100. The second assay was a neutralization ELISA carried out in 96-well plates or 3-cm diameter dishes (Hörling *et al.,* 1992). This was used to measure infectivity loss relative to attachment and internalization of virus that were assayed in the same format. The incubated virus–Mab mix (100 μl) was inoculated onto washed MDCK 96-well monolayers (Gibco) and incubated for 25 min at 4°C. After rinsing, 100 μl of warm DMEM, 1% HIFCS, 2 mM glutamine, and 20 μg/ml gentamicin were added, and the plate was incubated overnight at 37°C in the absence of trypsin, so that there was replication only within the original infected cell. Cells were then fixed with 2% paraformaldehyde in PBS and blocked with 3% BSA in TBS (0.02 M Tris–HCl, 0.14 M NaCl, pH 7.6) for 90 min at 20°C. *De novo* expressed HA on the cell surface was assayed as a measure of virus replication and detected with monoclonal mouse anti-HA IgA (H37-66-1), an anti-IgA alkaline phosphatase conjugate (Sigma), and DNPP. The product was read on an optical plate reader (Titertek Multiscan Plus; Life Sciences International) at 405 nm, where the virus control had an OD of approximately 1.1. All virus–antibody mixtures used in neutralization and all other assays were vortexed for 30 s immediately before inoculation onto cells, to break up any aggregates (Armstrong and Dimmock, 1992).

ELISA for virus attachment

Virus was neutralized and monolayers in 96-well plates inoculated exactly as described above. After nonattached virus was removed with cold DMEM, attached virus was fixed and permeabilized with cold methanol and blocked with 3% BSA in TBS overnight at 4°C. Attached virus was detected using an NP-specific Mab (HB-67, IgG1) in 1% BSA in TBS containing 0.1% Tween (Sigma). The NP antibody was then detected with rabbit anti-mouse IgG1 (Dako, Ely, UK), goat anti-rabbit alkaline phosphatase conjugate (Dako), and DNPP. The product was read as described above. As a negative control, cells were treated twice before virus inoculation with *Clostridium perfringens* neuraminidase type V (Sigma; 0.025 U for 10 min at 37°C) to remove *N*-acetylneura-

minic acid (NANA) receptors. Neutralization by ELISA was determined in the same system at the same time.

ELISA of the internalization of virus by cells

A virus–Mab mix containing 1500 HAU/ml was incubated for 60 min at 37°C, to allow neutralization to occur. The mix (100 μl) was inoculated onto a washed MDCK monolayer in a 96-well plate and incubated for 25 min at 4°C. After washing with cold DMEM, monolayers were incubated with warm DMEM at 37°C for 30 min to allow the attached virus to be internalized. Noninternalized virus was removed by treating the monolayer twice with 0.025 U of *C. perfringens* neuraminidase for 10 min at 37°C. Monolayers were then permeabilized by freeze–thaw cycle three times and fixed in −20°C methanol in saline for 30 min. After washing in TBS–Tween, monolayers were blocked with 3% BSA in TBS overnight at 4°C. Virus was detected as virion NP antigen as described above. To show that virus was being internalized by receptor-mediated endocytosis, we used conditions that are known to inhibit this process: either 4°C (Matlin *et al.,* 1981; Richman *et al.,* 1986) or incubating cells in hypertonic medium (0.45 M sucrose in medium) for 30 min at 20°C before inoculation of virus. This latter condition prevents the clathrin lattice formation required for receptor-mediated endocytosis (Daukas and Zigmond, 1985; Heuser and Anderson, 1989). Virus internalization and neutralization were determined in exactly the same 96-well system. Neutralization was determined by ELISA in the same system at the same time. Internalization data relate only to virus that attached to cells, and these were determined in the same cell culture system as described above.

Assay for virus–cell fusion using virus labeled with octadecyl rhodamine B chloride (R18)

Freshly purified virus (1.25×10^7 HAU in 500 μl) was mixed with 5 μl of R18 (85.5 μM; Molecular Probes Europe BV, Leiden, The Netherlands) for 60 min at 20°C in the dark. After centrifuging to remove any precipitate, free R18 was removed by pelleting virus through 20% sucrose at 110,000 *g* for 90 min. Virus was resuspended in 100 μl of PBS and stored at −70°C. Solubilization of R18-labeled virus in 1% Triton X-100 (BDH) gave a 150-fold increase in fluorescence, indicating that the R18 was self-quenched and incorporated into the virus lipid bilayer. For assay of fusion, nonneutralized virus or neutralized R18-labeled virus (200 HAU in 100 μl) was inoculated onto a 3-cm-diameter monolayer of MDCK or BHK cells for 25 min at 4°C. Unbound virus was removed with cold DMEM, and 200 μl of warm DMEM was added for 30 min at 37°C. Cells were again washed with cold DMEM and detached from the plastic by incubation with cold versene for 5 min at 20°C and scraping. These were pelleted and fixed by resuspending in cold 2% paraformaldehyde in the dark. Fluorescence was determined using a Luminescence Spectrophotometer LS-5 (Perkin–Elmer, Beaconsfield, UK), exciting at 560 nm and emitting at 590 nm, with an emission slitwidth of 10 nm. To demonstrate the specificity of the fluorescent signal, cells inoculated with R18-labeled virus either were kept at 4°C to inhibit fusion (Matlin *et al.,* 1981; Richman *et al.,* 1986) or were treated prior to infection with 500 nM bafilomycin A1 from *Streptomyces griseus* (Calbiochem: Novabiochem (UK), Beeston, UK) for 90 min at 37°C. Bafilomycin inhibits V-ATPase and prevents the acidification of endosomal vesicles, required to trigger HA-mediated fusion (Palokangas *et al.,* 1994; Ochiai *et al.,* 1995). Fusion data were calculated relative to the percentage of virus that attached to cells, measured in the same system. This was done by determining the amount of attached virus relative to the nonneutralized virus control from the fluorescent signal obtained after treatment with Triton X-100. The fusion ability of neutralized virus was calculated as a percentage of that achieved by the nonneutralized virus control. To keep the assays comparable, fusion and neutralization by ELISA were determined in the same 3-cm-diameter dish system at the same time. The neutralization assay was carried out exactly as the normal 96-well ELISA, except that the volumes were scaled up. The colored product was then transferred to 96-well plates for reading.

Assay of the affinity of Mabs and their Fab fragments for virions using surface plasmon resonance

The method was based on our earlier data (Schofield and Dimmock, 1996). Initially HA-specific monoclonal H37 IgG was covalently bound to a CM5 biosensor chip of a BIAcore 2000 (Biacore AB) by amine coupling. Any Mab bound nonspecifically was removed with 0.05 M triethylamine (Sigma). Purified virus (320 HAU in 40 μl) was suspended in 100 mg/ml CM5 dextran in HEPES-buffered saline (HBS; Fluka: Sigma), to prevent nonspecific interactions, and was captured on to the chip via the H37 IgG. The signal from the blank control, lane 1, is subtracted from the signal in lane 2, so that bulk refractive index changes are minimized and the sensorgram shows actual binding events. Approximately 700 refractive units (RU) of virus was bound and used for kinetic analysis of Mabs and Fabs. Kinetic measurements for each Mab and Fab pair were made simultaneously at 25°C on the same chip surface to minimize the effect of surface differences on kinetics. At least three different antibody concentrations were used. Antibody in HBS containing 10 mg/ml CM5 dextran was injected over lanes 1 and 2 at a flow rate of 20 μl/min and a dissociation time of 600 s. Afterward the chip surface was regenerated back to the covalently coupled Mab H37 by eluting bound virus with 0.05 M triethylamine. Kinetics of the binding of the Mabs and Fabs was analyzed using

the BIA evaluation software package (version 2.2). Data were analyzed by fitting each concentration of antibody to a Langmuir 1-to-1 binding model. Initially, the off-rate (k_d) was calculated by selecting 300 s of dissociation data (kept constant to compare Mabs and Fabs) and this rate was used along with the analyte concentration in moles to determine the on-rate (k_a). The equilibrium dissociation constant is k_d/k_a.

Data analysis

Dose–response curves were calculated by nonlinear regression analysis using Prism Graphpad software. To determine whether they were significantly different, we compared the complete curves using an unpaired *t* test, where a value of $P < 0.05$ is considered significant.

ACKNOWLEDGMENTS

M.J.E. was supported by a studentship from the BBSRC. We thank Dr. Walter Gerhard (The Wistar Institute, Philadelphia, PA) and Dr. Robert G. Webster (St. Jude Children's Research Hospital, Memphis, TN) for their generous gifts of hybridomas and Mabs, Dr. Wendy Barclay (University of Reading, UK) for the MDCK cells, and Dr. Ian Campbell (BIAcore AB) for advice on affinity measurements. Antibody work in the NJD laboratory was supported by grants from the National Heart, Lung, and Blood Institute, NIH (5R01HL59726) and The WPH Charitable Trust, UK.

REFERENCES

Armstrong, S. J., and Dimmock, N. J. (1992). Neutralization of influenza virus by low concentrations of HA-specific polymeric IgA inhibits viral fusion activity but activation of the ribonucleoprotein is also inhibited. *J. Virol.* **66,** 3823–3832.

Blumenthal, R., Bali-Puri, A., Walter, A., Covell, D., and Eidelman, O. (1987). pH-dependent fusion of vesicular stomatitis virus with Vero cells. *J. Biol. Chem.* **262,** 13614–13619.

Bullough, P. A., Hughson, F. M., Skehel, J. J., and Wiley, D. C. (1994). Structure of influenza haemagglutinin at the pH of membrane fusion. *Nature* **371,** 37–43.

Caton, A. J., Brownlee, G. G., Yewdell, J. W., and Gerhard, W. (1982). The antigenic structure of the influenza virus A/PR/8/34 hemagglutinin (H1 subtype). *Cell* **31,** 417–427.

Centers for Disease Control and Prevention. (1998). Update: Isolation of avian influenza A (H5N1) viruses from humans—Hong Kong, 1997–1998. *M.M.W.R. Morb. Mortal. Wkly. Rep.* **46,** 1245–1247.

Daukas, G., and Zigmond, S. H. (1985). Inhibition of receptor-mediated but not fluid-phase endocytosis in polymorphonuclear leukocytes. *J. Cell Biol.* **101,** 1673–1679.

Dimmock, N. J. (1993). Neutralization of animal viruses. *Curr. Top. Microbiol. Immunol.* **183,** 1–149.

Dimmock, N. J., Taylor, H. P., and Carver, A. S. (1984). Interaction of neutralized influenza virus avian and mammalian cells. *In* "Segmented Negative Strand Viruses" (R. W. Compans and D. H. L. Bishop, Eds.), pp. 355–359. Academic Press, London.

Ghendon, Y. (1990). The immune response to influenza vaccines. *Acta Virol.* **31,** 295–304.

Haddad, R. W., and Hutt-Fletcher, L. M. (1989). Depletion of glycoprotein gp85 from virosomes made with Epstein–Barr virus proteins abolishes their ability to fuse with virus receptor-bearing cells. *J. Virol.* **63,** 4998–5005.

Harlow, E., and Lane, D. (1988). "Antibodies: A Laboratory Manual." Cold Spring Harbor Laboratory Press, Cold Spring Harbor, NY.

Hernandez, L. D., Hoffman, L. R., Wolfsberg, T. G., and White, J. M. (1996). Virus-cell and cell-cell fusion. *Annu. Rev. Cell Dev. Biol.* **12,** 627–661.

Heuser, J. E., and Anderson, R. G. W. (1989). Hypertonic media inhibit receptor-mediated endocytosis by blocking clathrin-coated pit formation. *J. Cell Biol.* **108,** 389–400.

Hörling, J., Lundkvist, A., Huggins, J. W., and Niklasson, B. (1992). Antibodies to Puumala virus in humans determined by neutralization test. *J. Virol. Methods* **39,** 139–147.

Hudson, L., and Hay, F. C. (1989). "Practical Immunology," 3rd ed. Blackwell Scientific, Oxford.

Kida, H., Yoden, S., Kuwabara, M., and Yanagawa, R. (1985). Interference with a conformational change in the HA molecule of influenza virus by antibodies as a possible neutralization mechanism. *Vaccine* **3,** 219–222.

Kingsford, L., Boucquey, K. H., and Cardoso, T. P. (1991). Effects of specific monoclonal antibodies on La Crosse virus neutralization: Aggregation, inactivation by Fab fragments, and inhibition of attachment to baby hamster kidney cells. *Virology* **180,** 591–601.

Lafferty, K. J. (1963). The interaction between virus and antibody. II. Mechanism of the reaction. *Virology* **21,** 76–90.

Lamarre, A., and Talbot, P. J. (1995). Protection from lethal coronavirus infection by immunoglobulin fragments. *J. Immunol.* **154,** 3975–3984.

Matlin, K. S., Reggio, H., Helenius, A., and Simons, K. (1981). Infectious entry pathway of influenza virus in a canine kidney cell line. *J. Cell Biol.* **91,** 601–613.

McInerney, T. L., McLain, L., Armstrong, S. J., and Dimmock, N. J. (1997). A human IgG1 (b12) specific for the CD4 binding site of HIV-1 neutralizes by inhibiting the virus fusion entry process, but b12 Fab neutralizes by inhibiting a post-fusion event. *Virology* **233,** 313–326.

Miller, N., and Hutt-Fletcher, L. M. (1988). A monoclonal antibody to glycoprotein gp85 inhibits fusion but not attachment of Epstein–Barr virus. *J. Virol.* **62,** 2366–2372.

Ochiai, H., Sinya, S., Hirabayashi, T., Shimizu, Y., and Terasawa, K. (1995). Inhibitory effect of bafilomycin A1, a specific inhibitor of vacuolar-type proton pump, on the growth of influenza A and B viruses in MDCK cells. *Antiviral Res.* **27,** 425–430.

Outlaw, M. C., Armstrong, S. J., and Dimmock, N. J. (1990). Mechanisms of neutralization of influenza virus vary according to IgG concentration. *Virology* **178,** 478–485.

Outlaw, M. C., and Dimmock, N. J. (1990). Mechanisms of neutralization of influenza virus on mouse tracheal epithelial cells by mouse monoclonal polymeric IgA and polyclonal IgM directed against the viral haemagglutinin. *J. Gen. Virol.* **71,** 69–76.

Outlaw, M. C., and Dimmock, N. J. (1993). IgG-neutralization of type A influenza viruses and the inhibition of the endosomal fusion stage of the infectious pathway. *Virology* **195,** 413–421.

Pak, C. C., Krumbiegel, M., and Blumenthal, R. (1994). Intermediates in influenza virus PR/8 hemagglutinin-induced membrane fusion. *J. Gen. Virol.* **75,** 395–399.

Palokangas, H., Metsikkö, K., and Väänänen, K. (1994). Active vacuolar H+ATPase is required for both endocytic and exocytic processes during viral infection of BHK-21 cells. *J. Biol. Chem.* **269,** 17577–17585.

Possee, R. D., and Dimmock, N. J. (1981). Neutralization of influenza virus by antibody: Attachment, uptake and uncoating of neutralized virus in chick embryo cells. *In* "Genetic Variation among Influenza Viruses, Vol. ICN–UCLA Symposium XXI" (D. P. Nayak and C. F. Fox, Eds.), pp. 473–480. Academic Press, London.

Possee, R. D., Schild, G. C., and Dimmock, N. J. (1982). Studies on the mechanism of neutralization of influenza virus by antibody: Evidence that neutralizing antibody (anti-haemagglutinin) inactivates influenza virus by inhibiting virion transcriptase activity. *J. Gen. Virol.* **58,** 373–386.

Richman, D. D., Hostetler, K. Y., Yazaki, P. J., and Clark, S. (1986). Fate of influenza A virion proteins after entry into subcellular fractions of LLC cells and the effect of amantadine. *Virology* **151,** 200–210.

Rigg, R. J., Carver, A. S., and Dimmock, N. J. (1989). IgG-neutralized

influenza virus undergoes primary, but not secondary uncoating *in vivo*. *J. Gen. Virol.* **70,** 2097–2109.

Schofield, D. J., and Dimmock, N. J. (1996). Determination of affinities of a panel of IgGs and Fabs for an enveloped (influenza A) virus using surface plasmon resonance. *J. Virol. Methods* **62,** 33–42.

Schofield, D. J., Stephenson, J. R., and Dimmock, N. J. (1997a). High and low efficiency neutralization epitopes on the haemagglutinin of type A influenza virus. *J. Gen. Virol.* **78,** 2441–2446.

Schofield, D. J., Stephenson, J. R., and Dimmock, N. J. (1997b). Variations in the neutralizing and haemagglutination-inhibiting activities of five influenza A virus-specific IgGs and their antibody fragments. *J. Gen. Virol.* **78,** 2431–2439.

Staudt, L. M., and Gerhard, W. (1983). Generation of antibody diversity in the immune response of BALB/c mice to influenza virus hemagglutinin. I. Significant variation in repertoire expression between individual mice. *J. Exp. Med.* **157,** 687–704.

Stegmann, T., Morselt, H. W. M., Scholma, J., and Wilschut, J. (1987). Fusion of influenza virus in an intracellular acidic compartment measured by fluorescence dequenching. *Biochem. Biophys. Acta* **904,** 165–170.

Stewart, P. L., Chiu, C. Y., Huang, S., Muir, T., Zhao, Y., Chait, B., Mathias, P., and Nemerow, G. R. (1997). Cryo-EM visualization of an exposed RGD epitope on adenovirus that escapes antibody neutralization. *EMBO J.* **16,** 1189–1198.

Taylor, H. P., and Dimmock, N. J. (1985). Mechanism of neutralization of influenza virus by secretory IgA is diffferent from that of monomeric IgA or IgG. *J. Exp. Med.* **161,** 198–209.

Tsurudome, N., Glück, R., Graf, R., Falchetto, R., Schaller, U., and Brunner, J. (1992). Lipid interactions of the hemagglutinin HA2 NH_2-terminal segment during influenza virus-induced membrane fusion. *J. Biol. Chem.* **267,** 20225–20232.

Ugolini, S., Mondor, I., Parren, P. W. H. I., Burton, D. R., Tilley, S. A., Klasse, P. J., and Sattentau, Q. J. (1997). Inhibition of virus attachment to CD4+ target cells is a major mechanism of T cell line-adapted HIV-1 neutralization. *J. Exp. Med.* **186,** 1287–1298.

Webster, R. G. (1998). Influenza: An emerging disease. *Emerg. Infect. Dis.* **4,** 436–441.

Wiley, D. C., Wilson, I. A., and Skehel, J. J. (1981). Structural identification of the antibody-binding sites of Hong Kong influenza haemagglutinin and their involvement in antigenic variation. *Nature* **289,** 373–378.

Wrigley, N. G., Brown, E. B., Daniels, R. S., Douglas, A. R., Skehel, J. J., and Wiley, D. C. (1983). Electron microscopy of influenza hemagglutinin–monoclonal antibody complexes. *Virology* **131,** 308–314.

Wrigley, N. G., Laver, W. G., and Downie, J. C. (1977). Binding of antibodies to isolated haemagglutinin and neuraminidase molecules of influenza virus observed in the electron microscope. *J. Mol. Biol.* **109,** 405–421.